LAWRENCE
LIVERMORE
NATIONAL
LABORATORY

UCRL-JRNL-224889

# Erosion/Redeposition Analysis of the ITER First Wall with Convective and Non-Convective Plasma Transport

J. N. Brooks, J. P. Allain, T. D. Rognlien

October 1, 2006

Physics of Plasmas

# Erosion/redeposition analysis of the ITER first wall with convective and non-convective plasma transport

J.N. Brooks[1], J.P. Allain[1], T.D. Rognlien[2]

[1] *Argonne National Laboratory, 9700 S. Cass Ave., Argonne IL 60439, USA*
[2] *Lawrence Livermore National Laboratory, Livermore CA 94551, USA*

Sputtering erosion/redeposition is analyzed for ITER [IAEA Report GA10FDR1-01-07-13(2001)] plasma facing components, with scrape-off layer (SOL) plasma convective radial transport and non-convective (diffusion-only) transport. The analysis uses the UEDGE code [T.D. Rognlien *et al*., J. Nuc. Mat. 196(1992)347] and DEGAS code [D.P. Stotler *et al*., Contrib. Plasma Phys. 40(2000)221] to compute plasma SOL profiles and ion and neutral fluxes to the wall, TRIM-SP code [J.P. Biersack, W. Eckstein, J. Appl. Phys. A34(1984)73] to compute sputter yields, and the REDEP/WBC code package [J.N. Brooks, Fus. Eng. Des. 60(2002)515] for 3-D kinetic modeling of sputtered particle transport. Convective transport is modeled for the background plasma by a radially varying outward-flow component of the fluid velocity, and for the impurity ions by three models designed to bracket existing models/data. Results are reported here for the first wall with the reference beryllium coating and an alternative tungsten coating. The analysis shows: (1) sputtering erosion for convective flow is 20-40 times higher than for diffusion-only but acceptably low (~0.3 nm/s) for beryllium, and very low (~.002 nm/s) for tungsten; (2) plasma contamination by wall sputtering, with convective flow, is of order 1% for beryllium and negligible for tungsten; (3) wall-to-divertor beryllium transport may be significant (~10-60% of the sputtered Be current); 4) tritium codeposition in redeposited beryllium may be high (~1-6 gT/400s pulse).

## I. Introduction

Plasma/surface interactions remain a critical lifetime/performance issue for ITER [1] and future fusion reactors. Extensive sputtering erosion/redeposition analyses has been performed by ourselves and others, e.g., as reviewed in Refs. 2-3, for various ITER plasma facing components and surface materials, generally predicting marginally acceptable low-Z material erosion lifetime, acceptable plasma contamination, and significant tritium/carbon codeposition. Most of these studies focus on the divertor response, and with scrape off layer (SOL) plasma transport assumed to be governed by diffusion processes only. Recent tokamak and linear plasma simulator data, e.g., [4-6], show a strong possibility for convective radial transport of particles and energy occurring in the ITER SOL plasma. This transport arises from intermittent rapidly propagating "blob" events which are the end result of edge/SOL plasma turbulence. Convective transport leads to higher plasma density in the far SOL, near the wall, and to much higher charge exchange particle flux to the first wall. It is thus important to assess convective flow regime erosion/redeposition for the wall and other plasma facing components. Recent work in this area has examined general effects of convection on a solid or liquid wall surface [7], and has analyzed detailed effects for an ignition tokamak design (FIRE) with a beryllium wall [8]. Results of a limited fluid study of beryllium sputtering and transport for ITER using a hydrogenic plasma subject to radial convection are given in Ref. 8.

Issues for the ITER reference design beryllium wall include erosion, material transport to the divertor and “baffle” surfaces, and tritium codeposition in redeposited material. Beryllium transport to the edge plasma ("edge plasma" = pedestal region just inside the separatrix) and core plasma, while not as critical as for a high-Z material, also needs evaluation. Results from this study are also needed for use in integrated studies of an ITER all-tungsten divertor, including mixed-material Be/W surface effects.

We also assess a tungsten coated main-chamber wall. Tungsten has major advantages compared to beryllium: (1) it would eliminate issues with T/Be codeposition; (2) if used with a tungsten divertor it would eliminate any mixed-material problems (e.g., formation

of low melting point alloys); (3) it extrapolates in sputter erosion lifetime to post-ITER devices (demonstration reactor, etc.). A key concern with tungsten is plasma contamination, and we examine this.

This study uses a coupled-code/model approach similar to Ref. 8, with major upgrade of an all-kinetic computation of impurity ion SOL transport. There remain, however, several model limitations, including non-perfect coupling/consistency of the fluid, neutral, and impurity transport codes. Another limitation is the ad-hoc nature of the models, to be described, for convective effects on impurity particle transport. However, the present results are believed sufficient to show clear trends and to indicate needed research.

## II. Plasma Edge Analysis

The UEDGE plasma fluid code [9,10] is used to obtain plasma solutions for the ITER SOL/edge plasma, with and without convective flow. UEDGE contains a flux-limited, self-consistent neutrals model that is solved simultaneously with the plasma equations. Using the basic UEDGE hydrogenic plasma solution, the DEGAS-2 Monte Carlo code [11] computes the detailed charge exchange energy spectrum to the wall. The UEDGE/DEGAS analysis and solutions for the present ITER cases is described in Ref. 9, and is briefly summarized here. Impurity radiation provides a very similar (factor of ~2) reduction in the peak divertor heat flux using either carbon (for the originally-studied carbon divertor option) or injected neon (for the W divertor option). The geometry and computational domain are shown in Figure 1.

The base case used for the ITER calculations has 100 MW input from the core into the edge region, split equally between ions and electrons. The ITER base case also uses a fixed-density boundary condition at the edge/core interface (such density assumed to be maintained as needed, for example by pellet fueling.) The anomalous radial diffusion coefficients for particles and electron/ion energy are D = 0.3 $m^2/s$ for density and $\chi_{e,i}$ = 1 $m^2/s$ for both ion and electron temperature.

The convective transport is modeled as a time-averaged, radially-varying convective component of the radial fluid velocity:

$$V_c(r) = V_1 \exp[-(r - r_{\max})/r_v] + C_1 \qquad (1)$$

where r is the local radial distance from the separatrix (normal to the magnetic flux surface). A maximum of $V_1$ = 70 m/s is used, with $V_c = V_1 + C_1$ at the UEDGE last computed poloidal magnetic flux surface, here taken as $\psi_{max}$ =1.034 (see Fig. 1), while $r_v$ =0.027 m, and $C_1$= -1.4 m/s. To model the ballooning nature of the turbulence, the convection is only applied to the outer half of the torus, except with $V_c$ = 0 for the 0.5 m poloidal region near the (bottom and more remote upper) X-points and in the outer divertor leg. The magnitude and profile of $V_c$ are in the range deduced from ALCATOR C-MOD and DIII-D data [5,6] and simulations of DIII-D edge turbulence [12].

The hydrogenic plasma profiles computed by UEDGE for diffusion-only transport, and diffusion plus convection are shown in Fig. 2 at the outer midplane. The UEDGE mesh and computation does extend inward beyond that shown in Fig. 2 to -5.3 cm inside the separatrix at the midplane where the core boundary conditions are set.

As shown in Fig. 2, a significant difference between the diffusion only case and the diffusion plus convection case is the higher SOL density with convection. This is largely the result of an increase in neutral density owing to the higher convective ion flux, which in turn produces a strong ionization source in the main-chamber SOL. This ionization source also reduces the ion and electron temperatures in the SOL.

ITER is designed with significant radial distance (far SOL) between the first wall and the secondary separatrix determined by the magnetic flux surface intersecting the second magnetic X-point at the top of the ITER plasma. Because the UEDGE solution used here only extends to the edge of the second separatrix (at about $\psi$ = 1.035), it is necessary to specify the plasma beyond this point to the beryllium or tungsten wall (see Fig. 1). For the sputtered material transport calculations, we extend the UEDGE solution 17 cm to the

wall in a similar manner as in Ref. 8, using an exponential decay model of plasma density and temperatures, with e-folding distances (density: $\lambda_n$ =1.8 cm, 3.7 cm for diffusion-only, and with-convection respectively; temperature: $\lambda_T$ =1.5 $\lambda_n$) obtained from the solution region, and with specified minimum density/temperatures at the wall. (The sputtering/transport results are not particularly sensitive to these far-SOL plasma model parameters).

## III. Wall sputtering

### A. Model

The first wall will be sputtered by $D^0$, $T^0$ charge exchange (CX) neutrals, arising from the entire edge/SOL region, and potentially by impinging ions. We compute CX sputtering using the particle flux and energy spectrum from the UEDGE/DEGAS results convolved with TRIM-SP energy-dependent sputter yields. The CX flux is roughly uniform along the outer wall. Because of this we compute wall sputtering for a uniform CX flux to the lower half of the outer wall, i.e., from the midplane to the lower boundary (baffle). Total sputtered currents, including ion sputtering to be discussed, are then extrapolated to the full outer wall. (We do not here treat the inner wall, but trends should be similar). At the surface, an incidence angle of 45° is used for sputter yields, which is about the average CX incidence angle. Angle-resolved calculations can be made in the future, as DEGAS runs with better statistics are available, e.g., as in Ref. 8, however this would not make a major difference to the present conclusions since there is a substantial CX flux with energies well above threshold sputtering energies. (The CX energies extend up to about 1 keV for both convective and non-convective cases).

It should be noted that the present neutrals calculation does not include the effect of any gas puff refueling; such refueling can cause high but localized CX erosion.

Wall sputtering by *ions* depends on plasma conditions at the wall, viz., electron and ion temperature, plasma density, sheath structure and potential, and also the magnetic field/wall-surface intersection angle. The latter actually varies substantially along the ITER first wall, and likewise for other tokamak designs. Also, as mentioned, plasma

parameters are uncertain at the wall. The approach here for the ion sputtering estimate is to take a mild worst-case, assuming: (1) ½ of the UEDGE computed ion flux to the "wall" (past last computed flux point) goes to the actual wall (the rest impinging on the baffle); (2) plasma temperatures $T_e = T_i = 10$ eV at the wall (possibly somewhat higher than actual); (3) sheath potential of 3kTe = 30 V with similar dual magnetic/electrostatic sheath structure as at the divertor. With this model, D-T ions impact the wall at about 50 eV with average incidence of 52° from the normal.

To account for erosion due to helium ions and trace impurity ions we assume a 5% $He^{+2}$ plasma fraction at the wall, and 0.1% $O^{+3}$ (using coronal equilibrium value at ~10 eV). Then, using TRIM-SP computed sputter yields for sheath analysis derived energies of ~100 eV $He^{+2}$, and ~150 eV $O^{+3}$, with 45° average incidence angles, the combined helium and oxygen ion contribution to both Be and W sputtering is found to be about 10%.

Finally, for wall sputtering by redeposited ions, we compute this using transport results, to be discussed, finding this also to be about a 10% effect.

**B. Sputter yields**

The Monte Carlo TRIM-SP code is used to compute sputter yields for beryllium and tungsten. This is a version of the TRIM code [13]. The TRIM-SP version uses an equipartition between the local Oen-Robinson inelastic energy loss model and the non-local Lindhard-Sharff inelastic energy loss model. The simulations for tungsten use a surface binding energy of 8.68 eV, and for beryllium 3.38 eV, based on the respective heats of sublimation.

Selected TRIM-SP results for tungsten (including energies higher than used in this study but in part applicable to the divertor) are compared with experimental data and shown in Fig. 3. Due to the highly efficient energy transfer, tungsten reaches unity self-sputtering near 1 keV and reaches a maximum at impact energies between 5-10 keV. Normal incidence experimental data with D bombardment is adjusted to 45-degree incidence by Yamamura's empirical formula [14] for comparison. The empirical relation uses fitting

parameters obtained from the literature for the factors $f$ and $\alpha_{opt}$ , where $\alpha_{opt}$ is the nominal incidence angle at maximum yield. Values of 1.29 and 2.62 are used for $\alpha_{opt}$ and $f$, respectively. Normal incidence data for self-sputtering is not modified, since the absolute yield does not vary more than a few percent between normal and 30-degree incidence. As shown, the simulations are a good match to the data.

Table I shows computed yields for trace ion sputter yields, as modeled per above discussion, for beryllium and tungsten.

**C. Wall erosion results**

Table II shows wall sputtered currents and erosion rates, for the cases with and without plasma edge convection (and without self-sputtering). For beryllium, sputtering contributions are about 40% from CX neutrals, 40% from D-T ions, and 10% from trace ions. For tungsten, the D-T ion energy is below threshold, so there is no fuel ion sputtering—all sputtering is due to CX neutrals plus about a 10% contribution from trace ion sputtering.

We observe that sputtering is much higher (~ x40 Be, x20 W) for the convective case. However, even for this case, the erosion rate is acceptable for the low duty factor (~1%) ITER. For example, for plasma operation of 1.2 $x10^7$ seconds (30,000 pulses of 400 s/pulse), beryllium sputter erosion would be about 4 mm, and tungsten erosion would be a negligible 0.02 mm. For a 1 mm erosion limit a beryllium wall would need recoating some 4 times, a feasible number. (Local areas might need more frequent recoating, due to peaking effects, as mentioned, from gas puffing caused CX erosion). However, if ITER conditions were extrapolated to a commercial reactor, with 75% availability, a 1 mm Be coating would last less than one month (with tungsten lasting 10's of years). Beryllium use therefore does not extrapolate post-ITER, while tungsten would have essentially no sputtering lifetime restriction. (Erosion from ELM's and other plasma transients would therefore be the rate-limiting erosion lifetime factor for tungsten, not sputtering).

## IV. Sputtered particle transport

### A. Model

We compute the transport of sputtered material to the wall, baffle, divertor, and edge plasma, using the REDEP/WBC 3-D kinetic Monte Carlo impurity transport code [3,15]. Here we assume that the comparatively low impurity density does not significantly alter the overall plasma profiles in the SOL.

The WBC kinetic computation, utilizing an ensemble of test particles for impurity transport, is useful because of the long impurity/plasma collision mean free paths over much of the SOL region. Also, WBC provides a more detailed treatment of thermal forces, charge state collision dependencies, friction forces, and boundary effects than necessarily provided by a fluid computation. The disadvantage of a kinetic computation is run time, found for this application to be about a factor of ten more than a fluid calculation (using the $WBC^+$ code, a part of the REDEP code package). We note that future studies using the kinetic approach would benefit from supercomputer implementation.

For the WBC computation, an impurity atom (Be or W) is launched at a random outer wall location from the midplane down to the wall/baffle interface. The atom is launched with velocity chosen from TRIM-SP-confirmed distributions of energy-truncated Thompson, cosine elevation angle. The atom undergoes elastic collisions with the plasma (found to be a minor effect in this SOL plasma regime), and electron-impact ionization. ADAS ionization rates are used for beryllium, and REDEP code package rate coefficients for tungsten, for species $W^0 \rightarrow W^{+10}$.

If ionized, the ion undergoes charge-changing and velocity-changing collisions with the plasma. (Charge-changing collisions are almost entirely electron impact ionization, with recombination computed, but found to be small for the present plasma solutions). Velocity-changing collisions are computed as described elsewhere and include an extended (non-disparate mass) Braginski treatment [15,16]. Briefly, the impurity ion collisions with the plasma ions are computed using the Fokker Plank treatment. This covers parallel friction of single-particle impurity ions with the background D-T plasma

flowing along the magnetic field lines, parallel velocity diffusion, and perpendicular velocity diffusion, these terms all being highly dependent on the impurity ion charge state. Friction, and "thermal" forces are implicit in kinetic collision computations.

The impurity ions flow along the net magnetic field lines, subject to: additional cross-field diffusion with reference 0.3 $m^2/s$ diffusion coefficient; convective motion to be described; along-magnetic-field acceleration per the UEDGE solution parallel electric field. For this application we are able to suppress computation of sub-gyro orbit motion, except very near surfaces.

The UEDGE magnetic field line grid is used in WBC, with some modifications near the baffle and divertor where WBC uses an approximate coordinate mapping scheme. WBC follows the 3-D ion motion. The plasma parameters are given in 2-D space at each UEDGE poloidal-space grid point, i.e., in the radial and poloidal directions, and are interpolated in WBC between grid points.

It is unclear from present experiments and theory how SOL plasma convective/blob transport would affect wall-sputtered impurity ions. In principle, a kinetic calculation with WBC or like code could be made using a time and space dependent convective model, should such model become available based on elucidated physics. For the present purposes we use three phenomenological models simulating a range of possible physics. For the plasma with convection case, the reference model is that the impurity ions are subject to the same radial convective velocity as the background plasma. This is implemented in WBC by adding a convective component to the ion radial distance moved in a time step $\Delta t$:

$$\Delta r = \Delta r_0 + V_C(r)\Delta t \pm \sqrt{D\Delta t} \qquad (2)$$

where $\Delta r_0$ is the change in radial distance in the absence of convection or anomalous diffusion (i.e., due only to non-turbulent collisions), $V_c(r)$ is as given in Eq. 1, D as

mentioned is the radial diffusion coefficient, and the plus or minus sign is chosen randomly per the Monte Carlo method.

The second impurity transport model is that there is no impurity convection, i.e., $V_c = 0$ in Eq. (2), but only diffusion. This, obviously, is also used for the plasma case with no convection. (The presence or absence of convection for the hydrogenic background from UEDGE uses a physically equivalent fluid model for the hydrogenic particle transport, but we retain the freedom to set these separately from that of the impurities).

The third model is a modification of the Pigarov *et al.* model [17] for carbon in DIII-D, in which model the *sign* of the impurity ion convection velocity changes depending on the ion charge state. The convection is inward (towards the separatrix) for low charge states and outward (towards the wall) for higher charge states. This model is based on the idea that the low charge states are produced in the outer plasma regions that get transported inward, whereas the higher charge states are born near the separatrix and thus move outward as for hydrogen. Inward convection of impurities is qualitatively supported by a reduced 2D edge turbulence/transport simulation using a single-fluid impurity model [7].

As modified here for beryllium or tungsten, the charge-dependent model for the impurity ion radial convection velocity is:

$$V_c^z = -V_c \text{ for } Be^{+1\rightarrow+2} \text{ and } W^{+1\rightarrow+5}, \text{ while} \qquad (3)$$
$$V_c^z = +V_c \text{ for } Be^{+3\rightarrow+4} \text{ and } W^{>+5}.$$

For boundary conditions WBC uses: (1) particles crossing into the upper midplane region (not many) are reflected downward; (2) a particle history terminates upon hitting a surface (wall, baffle or divertor), or crossing the separatrix.

For each material and condition, the code uses 100,000 particle-histories per run.

**B. Transport Results**

Table III summarizes redeposition parameters for the plasma convection case with the reference impurity convection model, and the diffusion-only case. Trends for the convection case are: beryllium atom ionization mean free paths are much longer than for tungsten, as expected from mass and rate coefficient differences. For both materials there is significant redeposition on the wall and baffle regions, with low to moderate average redeposition energy. There is about a 10% flow of sputtered beryllium from the wall to the divertor. There is very little flow (0.6%) of beryllium to the edge plasma (across the separatrix). There is zero flow (within numerical limits) of tungsten to the divertor or across the separatrix.

For the diffusion-only plasma case we see the following trends: Ionization mean free paths are longer than for the convection case, due to lower near-wall plasma densities. Due to this and to the lack of convective force, there is much less redeposition on the wall, and higher transport to the divertor. Average energies of impinging ions on the divertor are higher. The higher energy is caused by several related factors, viz., higher plasma temperatures in the divertor region, higher ion charge states, higher ion temperature gradient force (for beryllium, less so for tungsten), and higher sheath acceleration. For beryllium the transport fraction to the edge plasma is higher than for the convective case, being about 8%, although as discussed above, the sputtered currents are much lower. For tungsten the edge plasma transport fraction remains negligible.

Tables IV and V show the effect of the three different impurity convection models on sputtered material transport. For the two "non-reference" models there is much less redeposition on the wall and more on the baffle. This clearly follows from the zero/lowered convection towards the wall, the only process causing wall redeposition then being diffusion which is a weak process. The increased beryllium flow to the divertor is significant in terms of formation of a beryllium overlayer or mixed Be/W divertor surface. Also, there is up to four times higher flow of beryllium to the edge plasma. For tungsten, there is very little flow to the divertor, in any of the convection model cases, and essentially no flow to the edge plasma.

Another case (not shown) was run for the convective plasma case, with increased diffusion coefficient for impurities of 1.0 $m^2/s$, compared to the reference 0.3 $m^2/s$. Focusing on the important parameter of transport to the edge plasma, the fraction for beryllium is about doubled, and for tungsten the fraction is still zero.

Finally, self-sputtering by redeposited ions at the wall is found—using the computed redeposited fluxes, energies, impingement angles—to be about a 10% effect for beryllium, and 20% for tungsten, for the convective plasma reference case. For the other cases, the effect is smaller due to lower wall redeposition rates.

**V. Plasma contamination**

Plasma contamination from first wall sputtering can occur by direct transport of wall material to the edge/core plasma and/or by re-sputtering of deposited material on the other surfaces (baffle, divertor). For tungsten, as discussed, the direct transport is negligible for the plasma solutions and models considered. This is due to the long distance (~25 cm) from the wall to the separatrix, with substantial plasma available to ionize sputtered tungsten atoms, and due also to the lack of a strong mechanism to transport tungsten ions across field lines to the plasma before they are convected to the baffle, wall, or divertor surfaces.

For the reference ITER baffle design, the phenomenon of re-sputtering of wall-originated tungsten would not affect plasma contamination, one way or the other, since the baffle surface is already tungsten, and since sputter properties of a redeposited metallic tungsten surface are essentially identical to the original coated surface. The same is true for the ITER "technology phase" tungsten-coated divertor. In addition, flow of wall-sputtered tungsten to the divertor is significant only for the non-convective plasma case.

Thus, a tungsten coated first wall appears to present no plasma contamination problem due to sputtering, for the conditions examined.

For beryllium, we can roughly assess the core plasma contamination potential by taking the impurity current to the edge, $I_z^{edge}$, as equal to the core plasma input current (a worst case), and using a global plasma particle confinement time, $\tau$, as a composite indicator of plasma impurity transport. ($I_z^{edge}$ is given by the product of the sputtered wall currents in Table II and the respective edge transport fraction). Then, the plasma impurity ion fraction, $f_z$, at equilibrium, is given by $f_z = I_Z^{edge}\tau/N_{DT}$, for total plasma D-T content $N_{DT}$. (This takes into account the largely non-recycling nature of a metallic impurity on the PFC surfaces). Using a ballpark estimate for ITER of $\tau$ = 10 s, and for $N_{DT}$ =1 x $10^{23}$, the core beryllium plasma concentration—-due to wall sputtering—is $f_z$ ~.01 (w/convection) and ~.004 (diffusion only). Thus, the plasma beryllium concentration for the reference case is of order 1%, a low amount. However, for the plasma convective case with the two alternative impurity convection models, the concentration could be about 3-4 times higher, which would be of concern, and this implies the need for more rigorous analysis in which the present codes are fully coupled to an edge/core plasma impurity transport code.

**VI. Tritium codeposition**

Hydrogen isotope trapping in redeposited beryllium is a strong function of surface temperature and plasma oxygen content/flux. A rigorous estimate requires a detailed convolution of spatially-dependent Be growth rate, local surface temperature, and estimate of beryllium-oxide vs. pure beryllium growth. This can be done if and when detailed thermal analysis of ITER surfaces becomes available, as is not presently the case. For scoping purposes, however, and following the considerations in Ref. 8, we can roughly assess the likelihood of tritium codeposition being a significant issue for ITER. We compute T/Be trapping assuming that all of the sputtered beryllium current (Table II) traps tritium via the redeposition process, using a fixed surface temperature of 250°, and using (D+T)/Be trapping rates of 0.3, and 0.05 for "abundant oxygen" and "low oxygen" assumptions, respectively [18,19]. This gives trapping rates of about 1 gT per 400 s pulse (low-oxygen) and 6 gT per 400 s pulse (abundant oxygen) for the convective case. For the diffusion only case, scaling with the sputtered beryllium current, the rate would be 38 times less. Therefore, tritium codeposition in wall-sputtered beryllium is a potentially

significant issue for the convective case, and detailed assessment is needed. (The T/Be codeposition, however, is likely to be easier to ameliorate than the analogous T/C situation arising from carbon divertor sputtering, e.g., see Refs. 2, 3, due to the more accessible locations of beryllium deposition, i.e., primarily on wall and baffle surfaces, and also the relative ease of tritium removal with moderate heating of the surface, again compared to carbon).

**VIII. Conclusions**

This study has assessed ITER first wall sputtering erosion with the critical plasma physics phenomenon of edge/SOL convective transport. The analysis uses coupled plasma/neutrals calculations, with full kinetic sputtered impurity transport, and detailed sputter yield computations. Convective plasma transport is predicted to result in much higher particle fluxes to the wall and consequently ~20-40 times higher sputtering than for diffusion-only radial physics. In spite of this increase, the erosion rate and plasma contamination potential of the reference beryllium coated wall appear to be acceptable for ITER, but both are high enough that ongoing analysis, with continuing improved models/codes/data is needed. Another key result is the significant wall to divertor beryllium transport; the implications of this on mixed-material generation/performance are being examined by us and colleagues for a tungsten divertor, and as pointed out Doerner [20], this transfer could significantly affect a carbon divertor, possibly being beneficial. Finally, for beryllium, the convective plasma regime introduces the potential for high T/Be codeposition rates, of order grams per pulse.

As other studies have noted, beryllium use does not extrapolate to a demonstration or commercial fusion reactor, due to short erosion lifetime. Because of this and the non-trivial plasma contamination and tritium codeposition issues, it would appear prudent to consider a tungsten coated wall for ITER, at least at some point in the experimental cycle. The key result here is that there is no predicted tungsten wall sputter erosion problem or plasma contamination problem. The low erosion is due to the well-known low sputter yields for D-T on tungsten, re-confirmed for this study using the predicted charge exchange energy spectrum, as well as the lack of high D-T ion or trace impurity ion

sputtering at the wall. Also, what little tungsten is sputtered from the wall does not make it into the edge plasma, due to the long distance to same and the lack of a strong inward transport mechanism. Of course, this result depends on uncertain and in some cases highly speculative models, in particular, the models for convective effect on impurity ions, and will need additional modeling, e.g., with coupling to core plasma codes, for reliable predictive computations.

As is well known, sputtering is only one issue for tungsten, other issues being disruption, ELMs and other plasma transient erosion, as well as blistering, flaking and other mechanical issues. However, the good predicted sputter erosion/transport tungsten performance is an encouraging result for ITER and future fusion reactors.

Future modeling plans include coupling of these results to the sputtering/transport of material to/from the baffle and divertor, improved code coupling, coupling to core plasma transport codes, use of space and time-dependent impurity convection models in WBC, and use of the extended capability of UEDGE [9] to simulate plasma solutions well into the far SOL gap region, include the baffle region above the divertor leg.

**Acknowledgements**
We thank M.E. Rensink (LLNL) for supplying DEGAS/ITER results. The originating developer of ADAS is the JET Joint Undertaking. This work was supported under the auspices of the U.S. Department of Energy (Office of Fusion Energy) at ANL and likewise by the University of California Lawrence Livermore National Laboratory under contract No. W-7405-Eng-48.

**References**

[1] ITER Technical Basis, Document GA10FDR 1-01-07-13 (2001), International Atomic Energy Agency (IAEA), Vienna

[2] G. Federici, C.H. Skinner, J.N. Brooks, *et al.*, Nuc. Fus. 41(2001)1967.

[3] J.N. Brooks, Fus. Eng. Des. 60(2002)515.

[4] G.Y. Antar , S.I. Krasheninnikov, P. Devynck, R.P. Doerner, E.M, Hollmann, J.A. Boedo, S.C. Luckhardt, R.W. Conn, Phys. Rev. Lett. 87(2001)6.

[5] J.A. Boedo, D.L. Rudakov, R.A. Moyer *et al.*, Phys. Plasmas 10(2003)1670.

[6] B. Lipschultz, D. Whyte, B. LaBombard, Plasma Phys. Control. Fus. 47(2005)1559.

[7] M. Kotschenreuther, T. Rognlien, P. Valanju, Fus. Eng. Des. 72(2004)169.

[8] J.N. Brooks, J.P. Allain, D.A. Alman, D.N. Ruzic, Fus. Eng. Des. 72(2005)363.

[9] T.D. Rognlien R.H. Bulmer, M.E. Rensink, J.N. Brooks, "Scrape-off layer plasmas for ITER with 2nd X-point and convective transport effects", PSI-17, J. Nuc. Mat. to be published.

[10] T.D. Rognlien *et al.*, J. Nuc. Mat. 196(1992)347.

[11] D.P. Stotler, C.F.F. Karney, M.E. Rensink, T.D. Rognlien, Contrib. Plasma Phys. 40(2000)221.

[12] T.D. Rognlien , M.V. Umansky, X.Q. Xu, R.H. Cohen, L.L. LoDestro, J. Nuc. Mat. 337-339(2005)327.

[13] J.P. Biersack, W. Eckstein, J. Appl. Phys, A34(1984) 73.

[14] Y. Yamamura, C. Mößner, H. Oechsner, Radiation Effects, 103(1987)25.

[15] J.N. Brooks, Phys. of Fluids 8(1990)1858.

[16] W.K. Terry, Phys. of Fluids B 2(1990)1944.

[17] A. Yu. Pigarov, E.M. Hollmann, S.I, Krasheninnikov, T.D. Rognlien, W.P. West, J. Nuc. Mat. 337-339(2005)371.

[18] M. Mayer, R. Behrish, H. Plank, J. Roth, G. Dollinger, C.M. Frey, J. Nuc. Mat. 230(1996)67; M. Mayer, J. Nuc. Mat. 240(1997)164.

[19] R.A. Causey, D.S. Walsh, J. Nuc. Mat. 254(1998)84; R.A. Causey, J. Nuc. Mat. 300(2002)91.

[20] R. Doerner, "The Implications of Mixed-Material Plasma Facing Surfaces", PSI-17, J. Nuc. Mat. to be published.

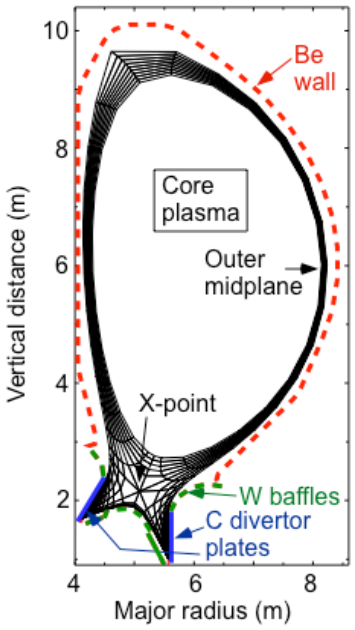


Figure 1. Poloidal cross-section of ITER edge region modeled showing the various material components of the wall/divertor. The ITER surfaces modeled are a first wall of ~700 $m^2$ area, "baffle" region of ~100 $m^2$ and divertor of ~50 $m^2$.

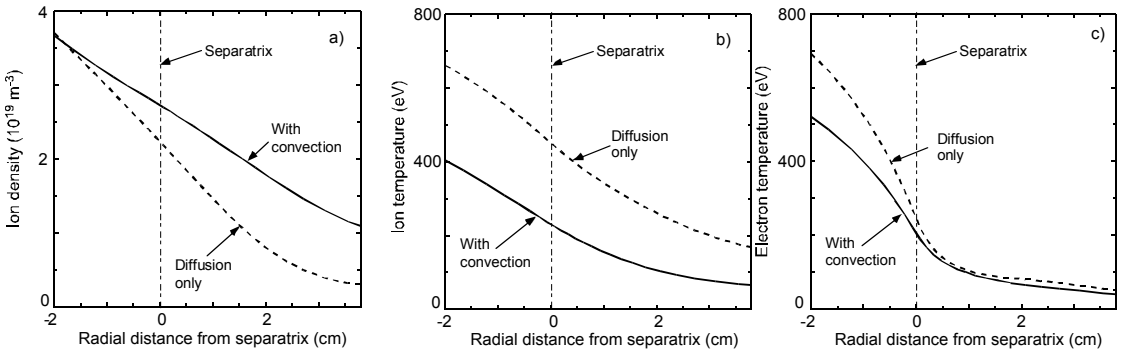


Figure 2. Plasma profiles at the outer midplane from UEDGE for hydrogen (50/50 DT mixture) only, with (solid line) and without (dotted line) convection from Eq. 1, The UEDGE domain ends at $\psi_{max}$ =1.034 just inside the second separatrix that forms from the upper, more distant X-point

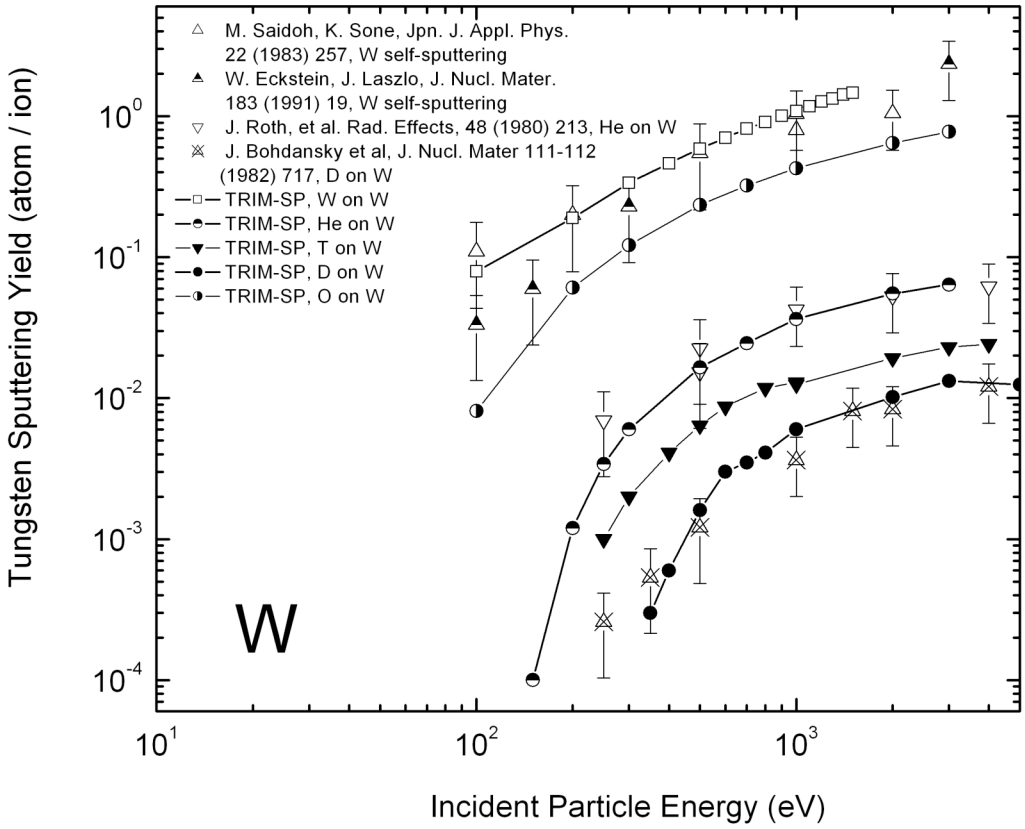


FIG. 3 Tungsten sputtering yield computational simulations with TRIM-SP compared to data. The yield is plotted against incident particle energy of D, T, He, O and W. The light particles are simulated at 45-degrees incidence and W at 30-degrees incidence with respect to the sample surface normal.

Table I. Sputtering from He and O on W and Be using TRIM-SP simulations with $10^5$ flights at 45-degree incidence.

| Sputter source | Be target | W target |
|---|---|---|
| 100 eV He | 0.1576 | 0.0000 |
| 150 eV O | 0.3983 | 0.0303 |

Table II. ITER first wall sputtering rates as a function of surface coating and edge plasma transport.

| Plasma case | Sputtered current[a]: **beryllium** $s^{-1}$ | **tungsten** $s^{-1}$ | Erosion rate[b]: **beryllium** m/s | **tungsten** m/s |
|---|---|---|---|---|
| With convection | $1.9 \times 10^{22}$ | $5.6 \times 10^{19}$ | $3.2 \times 10^{-10}$ | $1.8 \times 10^{-12}$ |
| Diffusion only | $5.0 \times 10^{20}$ | $2.8 \times 10^{18}$ | $8.3 \times 10^{-12}$ | $9.0 \times 10^{-14}$ |

[a] from total outer first wall
[b] w/o gas puffing

Table III. Transport of sputtered wall material; WBC code 100,000 histories/run.

| Parameter[a] | Plasma: with convection **beryllium**[b] | with convection **tungsten**[b] | diffusion only **beryllium** | diffusion only **tungsten** |
|---|---|---|---|---|
| Ionization mean free path[c], cm | 11.5 | 3.4 | 16.8 | 9.2 |
| Fraction to wall | .283 | .753 | .007 | .072 |
| Fraction to baffle | .617 | .247 | .304 | .705 |
| Fraction to divertor | .093 | $1.2 \times 10^{-4}$ | .614 | .224 |
| Fraction to edge plasma | .006 | 0 | .075 | $2.4 \times 10^{-4}$ |
| Charge state to wall | 1.4 | 3.2 | 1.1 | 3.1 |
| Charge state to divertor | 2.1 | 6.9 | 2.4 | 10 |
| Energy to wall, eV | 61 | 148 | 63 | 149 |
| Energy to baffle, eV | 118 | 515 | 187 | 519 |
| Energy to divertor, eV | 273 | 2326 | 766 | 3464 |

[a] unless otherwise indicated, average for redeposited ions
[b] with reference impurity convection model
[c] for sputtered atoms, normal to surface

Table IV. Transport as a function of impurity convection model; plasma with convection, **beryllium** wall.

| Sputtered particle convection model | Sputtered particle fraction to: Wall | Baffle | Divertor | Edge plasma |
|---|---|---|---|---|
| Same as plasma | .283 | .617 | .093 | .006 |
| No convection | .015 | .724 | .246 | .015 |
| Charge state dependent | .025 | .471 | .480 | .023 |

Table V. Transport as a function of impurity convection model; plasma with convection, **tungsten** wall.

| Sputtered particle convection model | Sputtered particle fraction to: Wall | Baffle | Divertor | Edge plasma |
|---|---|---|---|---|
| Same as plasma | .753 | .247 | $1.2 \times 10^{-4}$ | 0 |
| No convection | .109 | .888 | .003 | $1 \times 10^{-5}$ |
| Charge state dependent | .106 | .876 | .018 | 0 |